

Growth and characterization of $\text{Zn}_x\text{Cd}_{1-x}\text{Se}/\text{Zn}_{x'}\text{Cd}_{y'}\text{Mg}_{1-x'-y'}\text{Se}$ asymmetric coupled quantum well structures for quantum cascade laser applications

W. O. Charles^{a)} and A. Shen

Department of Electrical Engineering, The City College and The Graduate Center of CUNY, New York, New York 10031

K. Franz and C. Gmachl

Department of Electrical Engineering, Princeton University, Princeton, New Jersey 08544

Q. Zhang

Department of Physics, The City College and The Graduate Center of CUNY, New York, New York 10031

Y. Gong and G. F. Neumark

Department of Applied Physics and Mathematics, Columbia University, New York, New York 10027

Maria C. Tamargo

Department of Chemistry, The City College of CUNY, New York, New York 10031

(Received 26 October 2007; accepted 24 March 2008; published 30 May 2008)

The authors report the growth of a II-VI $\text{Zn}_x\text{Cd}_{1-x}\text{Se}/\text{Zn}_{x'}\text{Cd}_{y'}\text{Mg}_{1-x'-y'}\text{Se}$ asymmetric coupled quantum well (asymmetric-CQW) structure that was used to investigate the active region of an intersubband electroluminescence structure designed for emission at $\lambda=4.5\text{ }\mu\text{m}$. Such a structure could comprise the active region of a quantum cascade laser. The results of photoluminescence and Fourier transform infrared spectroscopy analysis show good agreement with the expected transition energies predicted by simulation results for the asymmetric-CQW structure. High resolution x-ray diffraction analysis indicates high structural quality of the sample and good control of the growth.

© 2008 American Vacuum Society. [DOI: 10.1116/1.2912085]

I. INTRODUCTION

Quantum cascade lasers (QCLs) that operate in the mid-infrared region are of great interest to the research community because of their potential application in areas such as infrared (IR) imaging and free space telecommunications. With this technology, it is possible to produce very narrow linewidth IR sources that are tunable. As a result, QCLs are ideal for chemical spectroscopy and hence could find applications in areas such as atmospheric pollution monitoring, medicine, and the military.

Since the first demonstration of the QCL in 1994,¹ there has been very significant progress in their design and fabrication. It is now possible to produce InGaAs/InAlAs lasers that operate at room temperature and deliver power in excess 500 mW and 1 W in continuous wave and pulse mode, respectively, within the 5–13 μm band.^{2–4} However, efforts to produce high performance QCLs in the 3–4 μm region with this material have not seen similar success. This is mainly due to fact that InGaAs/InAlAs lattice matched to InP has a conduction band offset (CBO) of 0.52 eV, which limits the emission wavelength to $\sim 4.3\text{ }\mu\text{m}$ (or 3.8 μm when strain compensation is used).^{5,6} Therefore, in order to cover the 3–5 μm atmospheric window, a material system with a larger CBO must be found.

Two of the leading alternative material candidates to date are the InAs/AlSb lattice matched to InAs substrates and

InGaAs/AlAsSb on InP substrates with CBOs of 2.1 and 1.6 eV, respectively.^{5,6} These materials are very promising because they possess a CBO that should permit emission in the entire mid-IR band. With these materials, QCLs with emission in the vicinity of 3 μm have been reported by several authors.^{5–7} While it is possible to adequately cover the 3–5 μm range of the mid-IR band with these materials, their performance is still not comparable to their InGaAs/InAlAs counterparts in the 5–13 μm range. In the case of InGaAs/AlAsSb, the lower performance may be due to the limitation of the effective CBO to 0.5 eV due to Γ -X intervalley electron leakage.⁸ Assuming that the photon energy of an efficient QCL is limited to $\sim \Delta E_c/2$, a high performance QCL with emission wavelengths in the 3–5 μm range cannot be achieved.⁵ With the InAs/AlSb material system on the other hand, the Γ -L intervalley scattering limits the effective CBO to 0.8 eV. Although, in this case, the CBO is large enough to produce QCLs in the 3–5 μm range, the laser performance still leaves much to be desired. The shortcomings of this material system may, in part, be due to the low thermal conductance of the InAs substrate and the relatively low confinement factor of the available laser waveguide.^{7,9,10} Given these shortcomings of the antimonides, the II-VI material system $\text{Zn}_x\text{Cd}_y\text{Se}/\text{Zn}_{x'}\text{Cd}_{y'}\text{Mg}_{(1-x'-y')}\text{Se}/\text{InP}$, with an effective CBO of 1.12 eV and the absence of Γ -X intervalley electron scattering, could be a viable alternative for producing high performance QCLs within the 3–5 μm atmospheric window.

^{a)}Electronic mail: wocharles99@aol.com

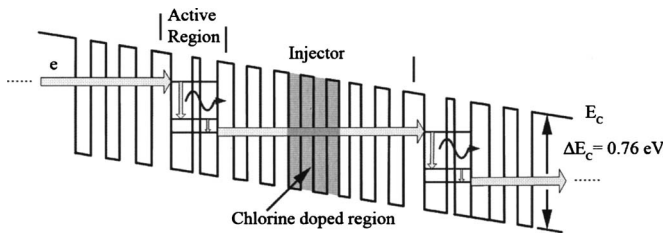


FIG. 1. Diagram of the conduction band edge of a structure illustrating the quantum cascade phenomenon as electrons traverse the active and injector region of an electroluminescence structure or a quantum cascade laser.

II. EXPERIMENT

In order to investigate the suitability of this material system for QCL fabrication, an electroluminescence (EL) structure was designed for emission at $4.5 \mu\text{m}$. In this design, the active region is composed of asymmetric coupled quantum wells (asymmetric CQWs) separated by digitally graded superlattice injector regions. The central region of the injector is doped to increase electrical conductivity and reduce the incidence of space charge buildup. Figure 1 is a schematic diagram of the EL structure. One period of the designed structure starting from the injection barrier is made up of the following layers in angstroms: **30/34/10/28/20/24/10/22/12/20/16/20/18/18/18/18/20/16/20/16/20/14/22/14/24/12/26/12** with the $\text{Zn}_{x'}\text{Cd}_{y'}\text{Mg}_{(1-x'-y')}\text{Se}$ barrier indicated in boldface and the Cl-doped layers underlined. The asymmetric-CQW region is shown in italics. This layer sequence could be repeated 30 times to make up the EL structure. As can be seen, the growth of the EL structure is a very time consuming and complex process. In order to understand its properties, the material quality and energy level distribution within the active region must be assessed and well established. To do this, a structure made up of asymmetric CQWs equivalent to the active region of the EL structure, but separated by simple quaternary barrier layers rather than injector regions was grown and investigated.

The asymmetric-CQW structure was grown by molecular beam epitaxy on (001) semi-insulating InP in a dual chamber Riber 2300P system. After deoxidation of the InP substrate in the III-V chamber, a $0.25 \mu\text{m}$ thick InGaAs buffer was grown at 400°C . The sample was then transferred via vacuum modules to the II-VI chamber where it was heated to 200°C . At this temperature, the InGaAs surface was exposed to a Zn flux for 40 s then a 10 nm ZnCdSe buffer layer was grown. At the end of this low temperature growth, the substrate temperature was raised to 300°C to complete the growth of the II-VI structure.¹¹

One period of the asymmetric-CQW structure starting from the spacer layer is made up of the following layers in angstroms: **190/34/10/28**. The barrier and spacer layers are shown in boldface while the Cl-doped well layers are underlined. The asymmetric CQWs were repeated 25 times and the wells were doped with chlorine ($n \sim 4 \times 10^{17} \text{ cm}^{-3}$). Doping is needed in order to observe intersubband absorption during Fourier transform IR (FTIR) spectroscopy. The multiple asymmetric-CQW structure was terminated with the growth

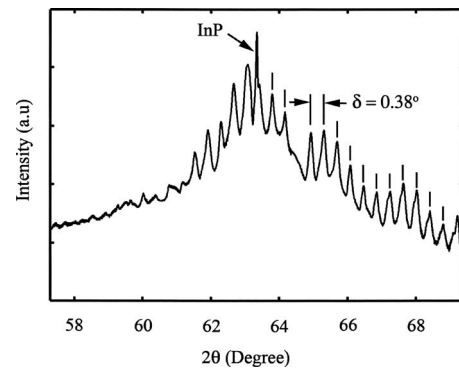


FIG. 2. High resolution x-ray diffraction curve for a $\text{Zn}_{0.43}\text{Cd}_{0.57}\text{Se}/\text{Zn}_{0.20}\text{Cd}_{0.19}\text{Mg}_{0.61}\text{Se}$ multiple asymmetric coupled quantum well structure consisting of 25 repeats.

of a 190 \AA ZnCdSe cap layer. In order to ascertain the growth conditions that would provide the desired doping levels and composition of the well and barrier layers, several calibration samples were grown. The carrier concentration of the doped thick-layer calibration samples was assessed using Hall effect measurements. The compositions of the well and barrier (or spacer) were determined by photoluminescence (PL) and x-ray diffraction to be $\text{Zn}_{0.43}\text{Cd}_{0.57}\text{Se}$ and $\text{Zn}_{0.20}\text{Cd}_{0.19}\text{Mg}_{0.61}\text{Se}$, respectively. This produced barrier and well band gaps of 3.03 and 2.08 eV, respectively, at 300°C . The effective CBO is estimated to be 0.76 eV (Ref. 12) which is comparable to the effective CBO of InAs/AlSb when Γ -L electron scattering is taken into account.

III. RESULTS AND DISCUSSION

In order to determine the material quality of the asymmetric-CQW structure, the sample was analyzed using PL and high resolution x-ray diffraction (HR-XRD). The large number of satellite peaks in the HR-XRD curve, shown in Fig. 2, indicates that the structural quality of the material is excellent. By using the satellite peaks separation (δ), the thickness of one period of the structure was calculated to be 270 \AA which is in good agreement with the nominal value of 262 \AA . This further indicates that there is good control of the well/barrier thickness. The absence of defect-related deep levels and the narrow linewidths of the PL spectra (67 meV at 300 K and 29 meV at 77 K) shown in Fig. 3 are indicative of good QW material quality and of QW thickness and composition uniformity. To determine the energy level distribution within the asymmetric-CQW structure the sample was polished into a multiple-pass waveguide geometry with 45° facets and analyzed using FTIR spectroscopy. During the FTIR measurements, the IR light from the Nexus 670 light source, was focused onto the sample using a ZnSe lens. The transmitted light for the waveguide was then focused onto an external mercury cadmium telluride detector. The results displayed in Fig. 4 suggest that the $\mathbf{e}_1 - \mathbf{e}_3$ and $\mathbf{e}_2 - \mathbf{e}_3$ absorption peaks occur at $\lambda = 4.13 \mu\text{m}$ and $\lambda = 5.18 \mu\text{m}$ corresponding to transitions energies 0.301 and 0.240 eV, respectively.

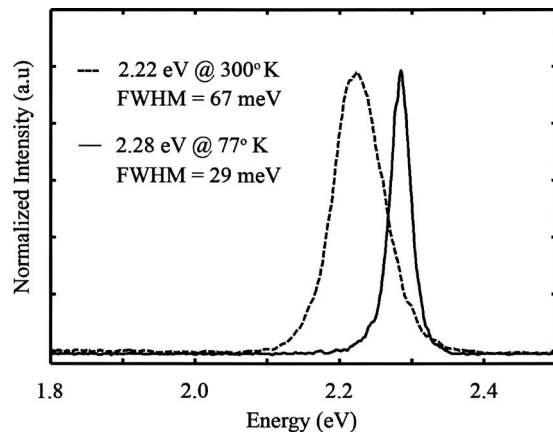


FIG. 3. Photoluminescence spectrum for the asymmetric coupled quantum well structure of Fig. 2. The FWHM at 300 and 77 K indicates that the material quality is very good. The emission energy is in very close agreement with that predicted by simulations.

These data indicate that the emission wavelength (e_2-e_3) of an EL structure grown with these asymmetric CQWs as active regions would be at about $5 \mu\text{m}$.

A simulation based on the envelope function approximation was performed to determine the room temperature energy level distribution within the asymmetric-CQW structure. The calculated e_1 , e_2 , and e_3 energy levels are 0.124, 0.171, and 0.437, respectively. By using this information, a comparison was made between the predicted and the measured transitions, and they are shown in Table I. A reasonable agreement between the predicted values and the measured values can be seen. From the FTIR results, the separation between e_1 and e_2 was calculated to be 0.061 eV. This value is somewhat larger than the design value of 0.047 eV, suggesting that our layers are slightly different in thickness than the design structure, and indicating that an adjustment of the growth parameters should be made prior to growth of the EL device structure. It is expected that during device operation,

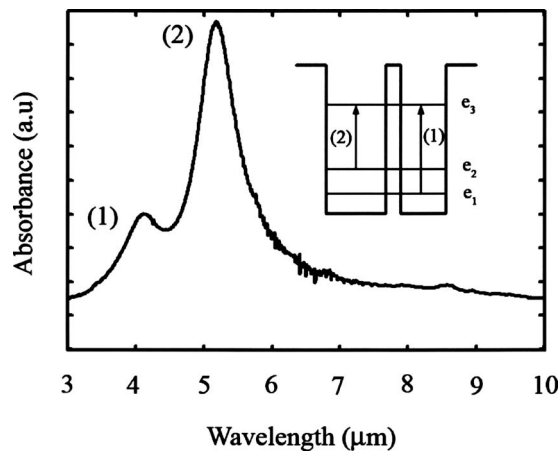


FIG. 4. FTIR spectrum for the asymmetric coupled quantum well structure of Fig. 2. The inset in the figure shows the electron transitions that result in the two peaks. The FTIR results suggest that: (1) $e_1-e_3=0.301 \text{ eV}$ or $\lambda=4.13 \mu\text{m}$, (2) $e_2-e_3=0.240 \text{ eV}$ or $\lambda=5.18 \mu\text{m}$.

TABLE I. Comparison between the calculated and measured energy transitions for an asymmetric-CQW structure.

Energy distribution	Predicted energy (eV)	Measured energy (eV)
PL (e_1-hh_1)	2.230	2.210
e_1-e_3	0.313 ($\lambda=3.97 \mu\text{m}$)	0.301 ($\lambda=4.13 \mu\text{m}$)
e_2-e_3	0.266 ($\lambda=4.67 \mu\text{m}$)	0.240 ($\lambda=5.18 \mu\text{m}$)
e_1-e_2	0.047	0.061 ^a

^aInferred from the two measured FTIR peaks.

the separation between e_1 and e_2 will be reduced to the desired separation of $\sim 30 \text{ meV}$ (approximately one LO phonon) when the complex injection barriers of the EL structure are used and a bias voltage is applied. A separation between e_1 and e_2 of approximately one LO phonon will ensure that population inversion between levels 2 and 3 will be achieved in a QCL structure.

IV. CONCLUSION

In conclusion, the FTIR results shown in Table I together with the PL and HR-XRD analysis confirm that high quality asymmetric CQWs can be grown and used as test samples to analyze the design and optical characteristics of proposed QCL structures before the complex and time consuming device growth is undertaken. We have also shown that using the design parameters of the asymmetric-CQW structure grown here, we should expect to fabricate an EL structure that emits at $\sim 5 \mu\text{m}$. To achieve shorter wavelengths, an optimized design of the active region will be needed.

ACKNOWLEDGMENTS

This work was supported by NSF Grant No. EEC-0540832 (MIRTHE-ERC) and NASA Grant No. NCC-1-03009 (COSI).

¹J. Faist, F. Capasso, D. L. Sivco, C. Sirtori, A. L. Hutchinson, and A. Y. Cho, *Science* **264**, 553 (1994).

²A. Evans, J. Nguyen, S. Slivken, J. S. Yu, S. R. Darvish, and M. Razeghi, *Appl. Phys. Lett.* **88**, 051105 (2006).

³A. Lyakh, P. Zory, D. Wasserman, G. Shu, C. Gmachl, M. D'Souza, D. Botez, and D. Bour, *Appl. Phys. Lett.* **90**, 141102 (2007).

⁴A. Evans, J. S. Yu, J. David, L. Doris, K. Mi, S. Slivken, and M. Razeghi, *Appl. Phys. Lett.* **84**, 314 (2004).

⁵J. Devenson, D. Barate, O. Cathabard, R. Teissier, and A. N. Baranov, *Appl. Phys. Lett.* **89**, 191115 (2006).

⁶D. G. Revin and J. W. Cockburn, *Appl. Phys. Lett.* **90**, 021108 (2007).

⁷J. Devenson, R. Teissier, O. Cathabard, and A. N. Baranov, *Appl. Phys. Lett.* **90**, 111118 (2007).

⁸Q. Yang, C. Manz, W. Bronner, K. Kohler, and J. Wagner, *Appl. Phys. Lett.* **88**, 121127 (2006).

⁹T. Borca-Tasciuc, D. Achimov, W. L. Liu, and G. Chen, *Proceedings of the International Conference on Heat Transfer and Transport Phenomena in Microscale*, Banff, Canada, 15–20 October 2000 (unpublished), p. 369–372.

¹⁰T. Borca-Tasciuc, D. W. Song, J. R. Meyer, and H. Lee, *J. Appl. Phys.* **92**, 4994 (2002).

¹¹H. Lu, A. Shen, M. C. Tamargo, W. Charles, I. Yokomizo, K. J. Franz, and C. Gmachl, *Appl. Phys. Lett.* **89**, 241921 (2006).

¹²M. Sohel, X. Zhou, H. Lu, M. N. Perez-Paz, M. C. Tamargo, and M. Munoz, *J. Vac. Sci. Technol. B* **23**, 1209 (2005).